IEICE TRANSACTIONS

on Electronics

DOI:10.1587/transele.2024DII0003

Publicized:2024/08/01

This advance publication article will be replaced by the finalized version after proofreading.

A PUBLICATION OF THE ELECTRONICS SOCIETY

The Institute of Electronics, Information and Communication Engineers
Kikai-Shinko-Kaikan Bldg., 5-8, Shibakoen 3chome, Minato-ku, TOKYO, 105-0011 JAPAN

Paper

Embedding Optical Components in Water to Make Aquatic Images Are Unaffected by Water Surface Undulations

Ryosuke Ichikawa†, Takumi Watanabe†, Hiroki Takatsuka†, Shiro Suyama†, and Hirotsugu Yamamoto†

SUMMARY We introduce a new aquatic display optical system based on aerial imaging by retro-reflection (AIRR). This system places passive optical components (a beam splitter and retro-reflector) in water to eliminate disturbances due to water motion. To demonstrate the effectiveness of the proposed optical system, we develop a prototype optical system and compensate for the motion of the water surface. We analyze the motion compensation and quantify its effectiveness using peak signal-to-noise ratio (PSNR) and structural similarity (SSIM) metrics.
From these results, we see that the optical system maintains a static image in water even when the water surface is undulating.
key words: *aerial display, aquatic display, aquatic image, retro-reflection, interface.*

1. Introduction

Aquatic display is a technology that forms images in water. Aquatic images formed by an aquatic display do not obstruct the flow of water or the movement of fish because no screen is installed. Because of this feature, aquatic displays are expected to be useful for experiments in the field of zoology, where computer graphics scenes are shown to fish to examine their behavior, and for fish farming in the field of fisheries science. We call this approach to zoology as VR biology.

One of the pioneering works in VR biology studied the effects of showing computer-simulated dots to medaka [1]. VR display of medaka induces real medaka to exhibit shoaling behavior. [2]. In both of these studies, a flat panel display was placed outside the water tank. In Ref. 3, researchers presented an omnidirectional aerial display for investigating optomotor reaction of medaka and flaring behavior of fighting fish [3].

Aerial imaging by retro-reflection (AIRR) [4] has a wide viewing angle and a high degree of freedom in its optical configuration. These features expand the possibilities of aerial display allowing to be used in all kinds of situations. Various studies have been conducted on AIRR, and it is being applied to other fields. For example, there is research on life-size large aerial displays combined with motion capture [5]. This report analyzes the visual distortion of acrylic panels mounted on a large aerial display and measures the aberration of the aerial image using a motion capture system. In other research, an aerial video-calling system has been proposed that allows users to make video calls while maintaining eye contact [6]. This video-calling system uses p-AIRR (polarization modulated AIRR) [7], taking advantage of the polarization encoding of the image to remove unwanted reflected light, and to provide more realistic communication than is possible with ordinary 2D displays. Furthermore, aerial imaging steganography has been proposed [8]. In other research, depth-fused 3D displays have been proposed that change the sense of depth by stacking displays [9]. In the field of theater production, proposals have been made for an aerial image to be perceived as if it tracked the observer using a hollow face illusion [10], and for an aerial teleprompter [11] that allows the user to read a script while facing forward.

Aquaculture and fisheries are an area where AIRR is expected to be utilized. We have realized the world-first aquatic display that forms information screen in water [12]. When displaying images in water, the air-water interface should be considered. Our previous paper reported the location of image formation due to refraction occurring at the air-water interface [13]. Another problem in showing images in water is image perturbation due to bubbles, and other unstable air-water interfaces. This problem causes unintentional motion in the visual stimuli and generates artifacts in VR biology experiments.

The purpose of this study is to realize an optical system designed to produce an aquatic image that is unaffected by fluctuation of water surface. Our proposed optical system has passive optical components installed underwater and does not contain the water-air surface boundary in the optical path. The effectiveness of our proposed optical system is investigated in comparison to an optical system that contains water-air surface boundary.

† The authors are with Utsunomiya Univ., Utsunomiya, 321-8585 Japan.

2. Principles

2.1 Principle of AIRR

Figure 1 shows the principle of AIRR. The AIRR optical system consists of three optical components: a light source, a beam splitter, and a retro-reflector. The light emitted from the light source impinges on the beam splitter and is divided into reflected and transmitted light. The reflected light then impinges in the retro-reflector and is retro-reflected. The retro-reflected light again impinges on the beam splitter and is divided into reflected and transmitted light. The transmitted light converges to form an aerial image. This aerial image appears at the plane-symmetrical position of the light source with respect to the beam splitter. Thus, the floating distance of the aerial image is determined by the distance between the light source and the beam splitter.

Figure 2 shows the principle of see-through AIRR [14]. In the AIRR shown in Fig. 1, the light source, beam splitter, and retro-reflector are set in a triangular configuration, while in see-through AIRR, the light source, beam splitter, and retro-reflector are arranged in a Z-shape. The basic principle is the same, but the difference is whether the reflected or transmitted light from the beam splitter is retro-reflected to form an aerial image. Another feature of see-through AIRR is the ability to observe the image from both sides. On the right side of Fig. 2, the aerial image can be seen as a real image, and from the left side, as a virtual image.

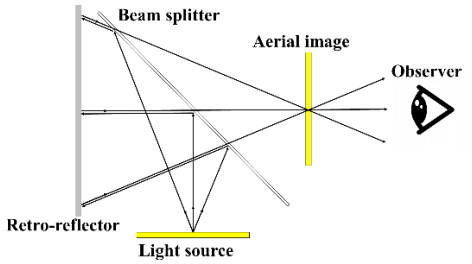

Fig. 1 Principle of aerial imaging by retro-reflection (AIRR).

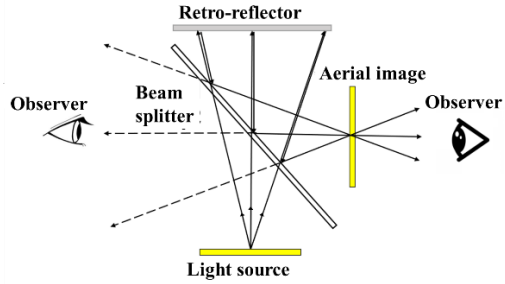

Fig. 2 Principle of see-through AIRR.

2.2 Principle of aquatic display using AIRR

Figure 3 shows the principle of aquatic display using AIRR. The major difference from standard AIRR is that, after the retro-reflected light beam reflects off the beam splitter, it is refracted at two points: the water tank outer and inner walls. The light emitted from the light source is divided by the beam splitter into reflected and transmitted light. The reflected light then impinges on the retro-reflector is retro-reflected. The retro-reflected light again impinges on the beam splitter and is divided into reflected and transmitted light. The transmitted light is refracted by the outer wall of the water tank and then again by the inner wall Then, the light converges to form an aquatic image.

An aquatic display can be implemented using both see-through AIRR and AIRR. Figure 4 shows the aquatic display principle using see-through AIRR. Similar to the see-through AIRR depicted in Fig. 2, the aquatic image can be perceived as a real image from one side and as a virtual image from the other side. Figure 5 shows the refraction due to the interface of the outer water tank. In general, the refractive index of air n_a is 1, that of glass n_β is 1.52, and that of water n_w is 1.33. Snell's law gives

$$n_\alpha \sin\alpha = n_\beta \sin\beta \quad (1)$$

where α is the incident angle from the atmosphere and β is the refraction angle on the water tank wall. Then, the refraction angle γ at the interface between the water and the water tank wall maintains the following relationship:

$$\alpha < \gamma < \beta. \quad (2)$$

Thus, due to refraction, the aquatic image is formed at a greater distance than the aerial image [15].

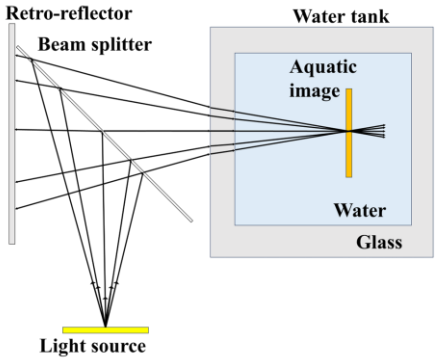

Fig. 3 Principle of aquatic display using AIRR.

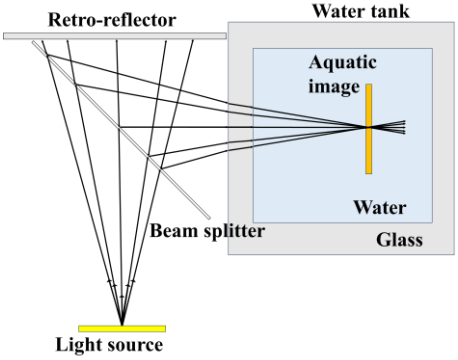

Fig. 4 Principle of aquatic display using see-through AIRR.

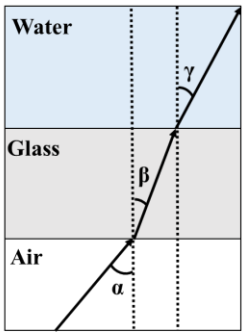

Fig. 5 Refraction by interface.

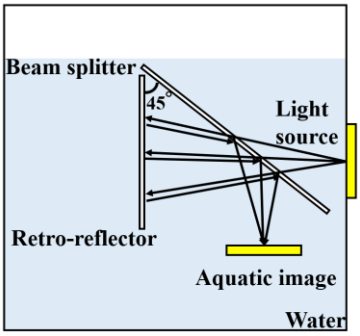

Fig. 7 Proposed optical system.

3. Optical system that forms an aquatic image above the water surface

3.1 Conventional optical system that forms an aquatic image through an air-water interface

Figure 6 shows a conventional optical system for aquatic image formation. The optical system is placed above the water surface. The optical system is based on the see-through AIRR shown in Fig. 2 in order to observe the fish through the beam splitter. The aquatic image thus formed is parallel to the water surface. The water surface is the interface between air and water in the ray path from the light source to the aquatic image. Undulations on the water surface affect the light rays.

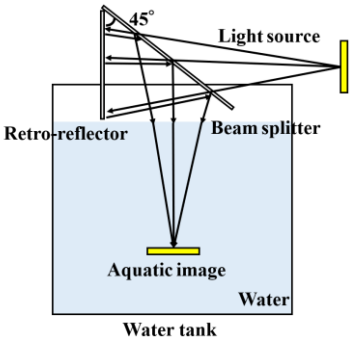

Fig. 6 Conventional optical system.

3.2 Proposed optical system that does not contain an air-water interface

Figure 7 shows a proposed optical system for aquatic image formation based on the see-through AIRR. The principle and structure are the same as that of conventional optical system as mentioned above. The innovative point is that the beam splitter and the retro-reflector are installed underwater. The light path from the light source to the aquatic image does not cross the air-water interface. All optical paths are in optically stable materials and are not affected by water surface undulations.

4. Compensating for water surface undulations

4.1 Experimental method

The effect of water surface undulations on the aquatic image was investigated in two scenarios: observing the aquatic image from within the water and from outside the water tank, using both the conventional optical system and the proposed optical system. The experimental equipment used is shown in Fig. 8. The light source was a 30 mm × 93 mm red LED badge. The displayed image, as shown in Fig. 9, was the letter A. The beam splitter was a 200 mm × 200 mm half mirror, and the retro-reflector was a 250 mm × 250 mm (Nippon Carbide Industries RF-Ax). The water tank was made of glass with walls 5 mm thick and 290 mm per side. The aquatic image was captured from the water using a GoPro HERO7. The aquatic image was captured from outside the water tank using a digital single-lens reflex camera (Nikon D5500).

The experimental setup for a conventional optical system is shown in Fig. 10. Figure. 10(a) shows the setup for underwater observation with the conventional optical system, and Fig. 10(b) shows the setup for observation from outside the water tank. The water height is set to 150 mm, and the distance from the light source to the beam splitter is 190 mm.

The experimental setup for the conventional optical system is shown in Fig. 11. Figure. 11(a) shows the setup for underwater observation with the proposed optical system, and Fig. 11(b) shows the setup for observation from outside the water tank. The water height is set to 250 mm, and the distance from the light source to the beam splitter is 100 mm.

In each case, images were captured with the water surface either still or undulating. The water surface undulations were produced by manually stirring the water to create waves with an amplitude of ± 1 cm. The experiment was filmed in dark surroundings.

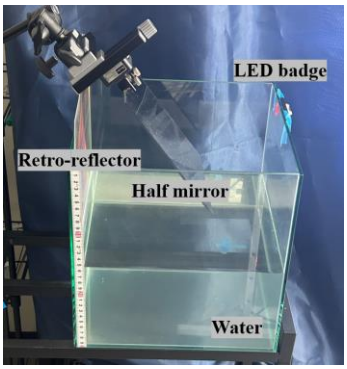

Fig. 8 Experimental environment.

Fig. 9 Displayed image on the LED badge.

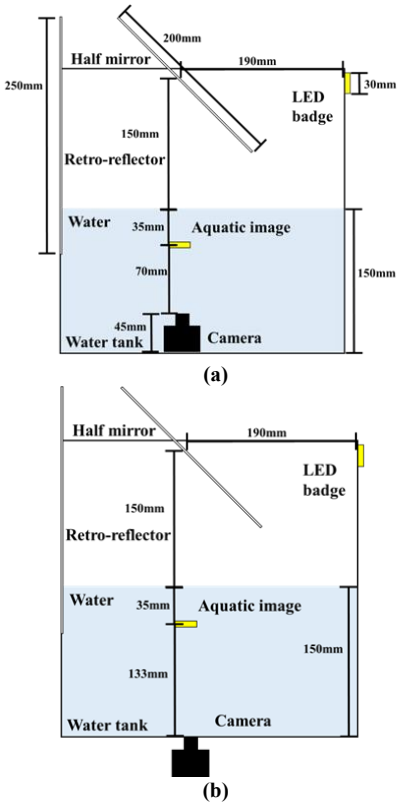

Fig. 10 Experimental optical system by use of conventional optics.
(a)Underwater observation, (b) Observation from outside the water tank.

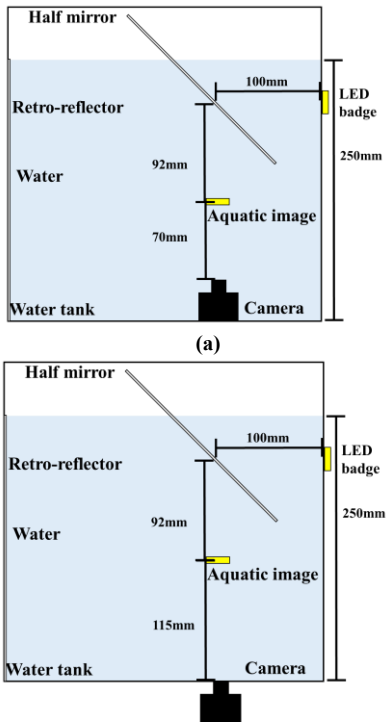

Fig. 11 Experimental optical system by use of proposed optics.
(a)Underwater observation, (b) Observation from outside the water tank.

4.2 Experimental results with conventional optics

Figure 12 shows underwater observation of the aquatic image and Fig. 13 shows observation of the aquatic image from outside the water tank. Figures 12(a) and 13(a) show the images when the water surface is quiet. Figures 12(b) and 13(b) show the images when the water surface is undulating. The image quality is worse when the water surface is undulating than when the water surface is quiet. The results of the in-water and out-of-water visibility imaging show that the conventional optics' aquatic image is affected by the water surface.

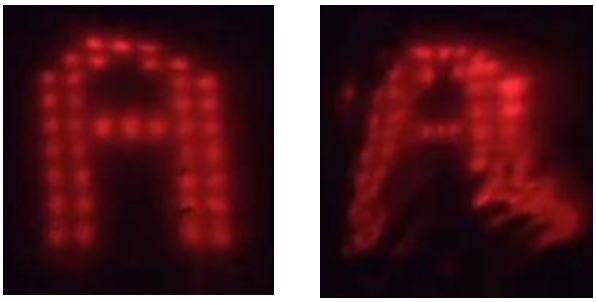

(a) **(b)**

Fig. 12 Underwater observation using conventional optics.
(a)Quiet state, (b)Undulating.

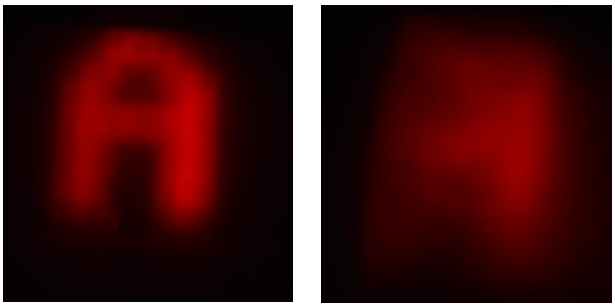

(a) (b)

Fig. 13 Observation from outside the water tank using conventional optics.
(a)Quiet state, (b)Undulating.

4.3 Experimental results with the proposed optical system

Figure 14 shows underwater observation of the aquatic image and observations of the aquatic image from outside the water tank is shown in Fig. 15. Figures 14(a) and 15(a) show the images when the water surface is quiet. Figures 14(b) and 15(b) show the images when the water surface is undulating.

There is no significant change in the aquatic image quality. The observation results of both in-water and out-of-water show that the aquatic image quality is not affected by the waves on the water surface. Thus, the proposed system is not affected by water surface undulations.

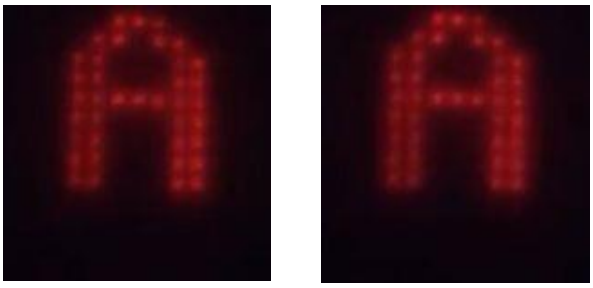

(a) (b)

Fig. 14 Underwater observation using proposed optics.
(a)Quiet state, (b)Undulating.

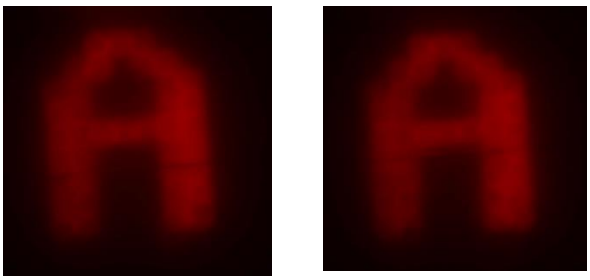

(a) (b)

Fig. 15 Observation from outside the water tank using proposed optics.
(a)Quiet state, (b)Undulating.

4.4 Quantitative evaluation of experimental results

To evaluate the impact of water surface disturbance on the aquatic image, we used peak signal-to-noise ratio (PSNR) [16]and structural similarity (SSIM) [17]. PSNR calculates the difference between the image and the brightness of each pixel in the image. The equations for PSNR can be expressed as:

$$\mathrm{PSNR} = 10 \cdot log_{10}\left(\frac{\mathrm{MAX}^2}{\mathrm{MSE}}\right) \tag{2}$$

where MAX refers to the maximum value that each pixel can take, 255 in this case: MSE indicates mean squared error between two images. SSIM quantifies the difference in brightness, contrast, and structure between the two images. The equations for SSIM can be expressed as:

$$\mathrm{SSIM}(x,y) = \frac{(2\mu_x\mu_y + c_1)(2\sigma_{xy} + c_2)}{(\mu_x{}^2 + \mu_y{}^2 + c_1)(\sigma_x{}^2 + \sigma_y{}^2 + c_2)} \tag{3}$$

where μ and σ indicate mean and standard deviation in the small window, respectively. σ_{xy} is the covariance of x and y. SSIM takes a value from 0 to 1. Both PSNR and SSIM become larger as the restored image gets closer to the original image. These values were calculated using Python.

The results of obtaining the PSNR and SSIM for the underwater observations with the conventional optical system (Figs. 12(a) and 12(b)) and the proposed optical system (Figs. 14(a) and 14(b)) are summarized in Table 1. The PSNR of the aquatic image observed with the conventional optical system is 17.64, whereas for the proposed optical system, it is 33.38. The proposed optical system shows a higher PSNR value, indicating better image quality. Regarding SSIM, the aquatic image captured with the conventional optical system has a value of 0.650, whereas that with the proposed optical system achieves 0.946. This suggests that in underwater observation, the proposed optical system not only achieves a higher PSNR but also demonstrates SSIM values closer to 1, indicating minimal impact on image fidelity.

The results of PSNR and SSIM obtained from observations outside the water tank using both the conventional optical system (Figs. 13(a) and 13(b)) and the proposed optical system (Figs. 15(a) and 15(b)) are summarized in Table 2. For observations from outside the water tank, the PSNR of aquatic image with the conventional optical system is 18.25, whereas with the proposed optical system, it is 30.16. The SSIM values show improvement with the proposed optical system, where the conventional system achieves 0.795 compared to 0.969 for the proposed system. This indicates that even when observed from outside the water tank, the proposed optical system has less impact on image quality.

These results demonstrate that the proposed optical system outperforms the conventional system in quantitative evaluation of aquatic image quality.

Table 1. PSNR and SSIM for the effect of water surface motion on the underwater observations.

	PSNR	SSIM
Conventional optics	17.64	0.650
Proposed optics	33.38	0.946

Table 2. PSNR and SSIM for the effect of water surface motion on observations from outside the water tank.

	PSNR	SSIM
Conventional optics	18.25	0.795
Proposed optics	30.16	0.969

5. Conclusion

By embedding passive optical components in water, we propose an optical system to form an aquatic image that is not affected by water surface undulations. We have developed a prototype optical system and captured images for each water surface condition. The captured aquatic images were compared using PSNR and SSIM to confirm the effectiveness of the proposed optics by comparing with an optical system that contains air-water interface. Our optical system maintains a static image in water even when the water surface is undulating.

Acknowledgments

A part of this work was supported by JSPS KAKENHI Grant Number 20H05702.

The authors with to thank Dr. Nathan Hagen who assisted in the proof-reading of the revised manuscript.

References

[1] W. Matsunaga, and E. Watanabe, "Visual motion with pink noise induces predation behavior," Sci. Rep., vol.2, p. 219 (2012).
[2] T. Nakayasu, and E. Watanabe, “Biological motion stimuli are attractive to medaka fish,” Anim. Cognit., vol.17, pp. 559–575 (2014).
[3] E. Abe, M. Yasugi, H. Takeuchi, E. Watanabe, Y. Kamei, and H. Yamamoto, "Development of omnidirectional aerial display with aerial imaging by retro-reflection (AIRR) for behavioral biology experiments," Opt. Rev., vol.26, pp. 221–229 (2019).
[4] H. Yamamoto, Y. Tomoyama, and S. Suyama, "Floating aerial LED signage based on aerial imaging by retro-reflection (AIRR)," Opt. Express, vol.22, pp. 26919–26924 (2014).
[5] M. Adachi, M. Yasugi, S. Suyama, and H. Yamamoto, "Method of acquiring shapes using motion capture of aerial images formed by large acrylic panels," Opt. Rev., vol.30, pp. 647–656 (2023).
[6] K. Fujii, N. Endo, N. Hagen, M. Yasugi, S. Suyama, and H. Yamamoto, "Aerial video calling system with eye-matching feature based on polarization-modulated aerial imaging by retro-reflection (p-AIRR)," Opt. Rev., vol.29, pp. 429–439 (2022).
[7] M. Nakajima, K. Onuki, I. Amimori, and H. Yamamoto, "Polarization state analysis for polarized aerial imaging by retro-reflection (PAIRR)," Proc. IDW 22, pp. 429–432 (2015).
[8] K. Fujii, M. Yasugi, S. Maekawa, H. Yamamoto, "Aerial imaging steganography method for aerial imaging by retro-reflection with dual acrylic ball," Opt. Rev., vol.29, pp. 250–260 (2022).
[9] Y. Terashima, S. Suyama, and H. Yamamoto, "Aerial depth-fused 3D image formed with aerial imaging by retro-reflection (AIRR)," Opt. Rev., vol.26, pp. 179–186 (2019).
[10] T. Watanabe, H. Takatsuka, S. Suyama, and H. Yamamoto, "Hollow Face Illusion Evoked Even by Binocular Vision of Aerial 3D Image," Proc. IDW 30, pp.1319–1322 (2023).
[11] D. Tasaki, H. Nobori, N. Kohara, K. Iwabuchi, M. Kobayashi, S. Shimomura, R. Ichikawa, T. Nishiyama, S. Hara, S. Suyama, S. Ito, F. Nakamura, J. Tanida, and H. Yamamoto, "Aerial Prompter Using AIRR That Allows the Performer and Audience to See the Script From Two Directions at the Same Time," Proc. DHIP 2023, P─18 (2023).
[12] D. Kudo, K. Chiba, M. Yasugi, and H. Yamamoto, "Measurement of Screen Position of an Aquatic Display," Proc. IDW 27, pp. 265–268 (2020).
[13] D. Kudo, M. Yasugi, N. Ninomiya, S. Suyama, and H. Yamamoto, "Reduction of converging distance change in an aquatic display formed with aerial imaging by retro-reflection in conjugated optical structure," Opt. Express, vol.31, pp. 10965–10977 (2023).
[14] R. Kakinuma, M. Yasugi, S. Ito, K. Fujii, and H. Yamamoto, " Aerial Interpersonal 3D Screen with AIRR that Shares Your Gesture and Your Screen with an Opposite Viewer," IMID 2018, Digest, p. 636 (2018).
[15] R. Ichikawa, K. Kishinami, D. Kudo, K. Fujii, M. Yasugi, S. Suyama, and H. Yamamoto, "Comparison of Imaging Distances for Underwater and Aerial Images by AIRR," IMID 2023, Digest, p. 767 (2023).
[16] Z. Wang, A. C. Bovik, H. R. Sheikh, and E. P. Simoncelli, "Image quality assessment: from error visibility to structural similarity," IEEE Trans. Image Process., vol. 13, 600–612 (2004).
[17] Deshpande, R.G., Ragha, L.L. and Sharma, S.K. "Video Quality Assessment through PSNR Estimation for Different Compression Standards," Indonesian Journal of Electrical Engineering and Computer Science, vol. 11, 918-924. (2018)

Ryosuke Ichikawa received his B. E. degrees from Utsunomiya University, Japan in 2024. Currently, he is doing a Master's degree in Utsunomiya University. His research interest includes an aquatic display using aerial imaging by retro-reflection (AIRR).
He was a recipient of Best Student Paper Award at IDW'23.

Takumi Watanabe received his B. E. degrees from Utsunomiya University, Japan in 2024. Currently, he is doing a Master's degree in Utsunomiya University. His research interests include eye-tracking aerial image using hollow face illusion and optical design for 3D object.
He was a recipient of Best Poster Awards at 3DSA 2023.

Hiroki Takatsuka received his B. E. and M. E. degrees from Utsunomiya University, Japan. Currently, he is a Ph. D. candidate at Utsunomiya University, Japan. His research interests include deep-learning assisted single-pixel-imaging and ultra-wide field-of-view display using aerial image. He was a recipient of Student Presentation Award at DHIP'22, Student Paper Award at IP2022 and Best Student Paper Award at IDW'23.

Shiro Suyama received the M.E. degrees from Kyushu University in 1981. Since joining NTT Electrical Communication Laboratories in 1981, he has been engaged in research and development on transistor and liquid-crystal devices. He received the PhD degree from Kyushu University in 1990. He was a Professor at Tokushima University from April 2007 to March 2021 and is currently a Project Professor at Utsunomiya University from April 2021. He is engaged in research on 3D display systems; e.g. DFD (Depth-fused 3-D) display, Arc 3D display, Aerial display, Enhancing image reconstruction in Brain, Three-dimensional perceptions and Liquid-crystal varifocal lens.

Hirotsugu Yamamoto received the B.E., M.E., and Ph.D. degrees from the University of Tokyo, Tokyo, Japan. After graduation, he joined the Department of Optical Science and Technology at University of Tokushima, Japan. From April 2014, he joined the Center of Optical Research and Education (CORE) at Utsunomiya University, where he is currently a professor at School of Engineering, Utsunomiya University. He has been a project leader for international standardization of aerial display at IEC/TC110, the chair of IEC/TC110 Japan Mirror National Committee, and received IEC1906 Award for his outstanding contribution. In April 2021, he has become a distinguished professor at Utsunomiya University.